Published online May 20, 2004

*Nucleic Acids Research, 2004, Vol. 32, No. 9* ***2901–2911***
*DOI: 10.1093/nar/gkh600*

# Clamping down on weak terminal base pairs: oligonucleotides with molecular caps as fidelity-enhancing elements at the 5′- and 3′-terminal residues

**Sukunath Narayanan, Julia Gall and Clemens Richert***

Institute for Organic Chemistry, University of Karlsruhe (TH), D-76131 Karlsruhe, Germany

Received March 23, 2004; Revised and Accepted April 19, 2004

## ABSTRACT

**The base-pairing fidelity of oligonucleotides depends on the identity of the nucleobases involved and the position of matched or mismatched base pairs in the duplex. Nucleobases forming weak base pairs, as well as a terminal position favor mispairing. We have searched for 5′-appended acylamido caps that enhance the stability and base-pairing fidelity of oligonucleotides with a 5′-terminal 2′-deoxyadenosine residue using combinatorial synthesis and MALDI-monitored nuclease selections. This provided the residue of 4-(pyren-1-yl)butyric acid as a lead. Lead optimization gave (*S*)-*N*-(pyren-1-ylmethyl)pyrrolidine-3-phosphate as a cap that increases duplex stability and base-pairing fidelity. For the duplex of 5′-AGGTTGAC-3′ with its fully complementary target, this cap gives an increase in the UV melting point $T_m$ of +10.9°C. The $T_m$ is 6.3–8.3°C lower when a mismatched nucleobase faces the 5′-terminal dA residue. The optimized cap can be introduced via automated DNA synthesis. It was combined with an anthraquinone carboxylic acid residue as a cap for the 3′-terminal residue. A doubly capped dodecamer thus prepared gives a melting point decrease for double-terminal mismatches that is 5.7–5.9°C greater than that for the unmodified control duplex.**

## INTRODUCTION

Oligonucleotide hybridization probes often have to find their target sequence in a sea of competing sequences. This is particularly true for the probes of DNA microarrays or 'DNA chips' (1–3). High-fidelity hybridization probes should bind their fully complementary target sequence tightly, while showing little affinity for partially matched competitor sequences. It is becoming increasingly clear, however, that cross-hybridization to non-target sequences is a serious problem when performing hybridizations with targets representing a substantial portion of entire genomes (4,5). The challenge is greatest when single-nucleotide resolution is required, either because the expression of genes from closely related families of proteins is to be monitored or because single-nucleotide polymorphisms are to be detected by hybridization (6,7). Resolving single-nucleotide differences requires a substantial drop in binding energy for every mismatched or absent base pair. This is easiest to achieve in the interior of duplexes, where a mismatch affects several neighboring base pairs and the aggregate loss in stability is substantial. For the termini, with their frequently fraying base pairs, the decrease in duplex stability caused by a single mismatch is smaller, however, making it particularly challenging to achieve single-nucleotide resolution at these sites. In fact, mismatched base pairs at the termini that involve as many hydrogen bonds as the canonical base pair, such as T:G wobble base pairs replacing a T:A base pair, have an almost imperceptible effect on duplex stability (8).

One approach to improving microarray experiments is to correct for false-positive and false-negative results after simulation of total hybridization equilibria (9). However, predicting the thermodynamic parameters for duplex formation with the required level of accuracy remains difficult (10). Instead, one might extend the length of the oligonucleotide probes, but the longer the sequence, the smaller the effect of a single mismatch on overall duplex stability, and the more likely that partial complementarity with other targets will lead to false-positive signals. Finally, one might improve base-pairing fidelity through chemical modifications. For primers used in enzymatic assays, the conjugation to minor groove binders has been reported to improve selectivity (11,12). Other approaches use folded probes (13–15) or backbone-modified oligonucleotides for high fidelity (16). Further, modified nucleobases are being employed to create 'isostable DNA' (17–19), whose melting point is independent of the sequence, so that universally stringent conditions for hybridization may eventually be established.

We have studied molecular 'caps', i.e. non-nucleic acid moieties covalently attached to the termini, as fidelity-enhancing elements (FEEs) that improve base-pairing fidelity at the termini. Bile acid residues linked to oligonucleotides via an amide bond have been found to increase duplex stability and base-pairing fidelity at the terminus for oligonucleotides with 5′-terminal thymidine and deoxycytidine residues (8,20–22). As schematically shown in Figure 1, stabilizing duplexes

*To whom correspondence should be addressed. Tel: +49 721 608 2091; Fax: +49 721 608 4825; Email: cr@rrg.uka.de

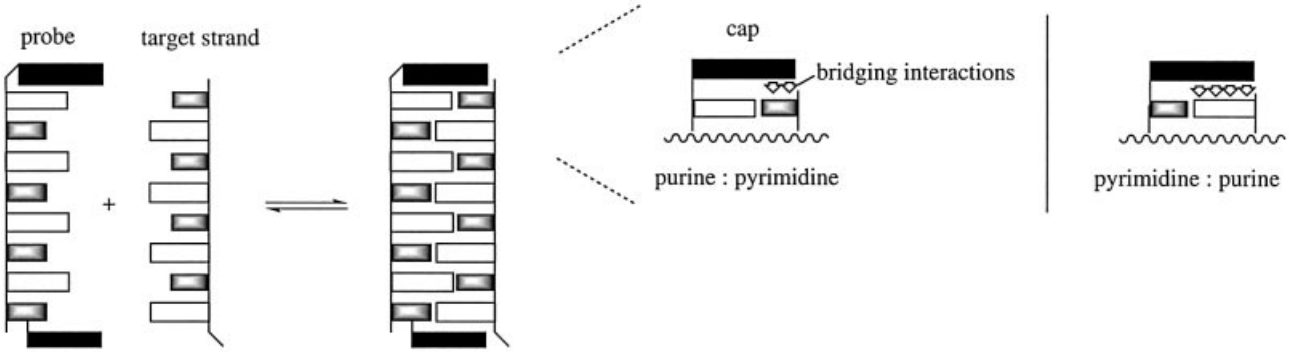


**Figure 1.** Schematic representation of a DNA duplex with molecular caps bridging the termini. The purines are shown as open rectangles, pyrimidines are gray rectangles and caps are black rectangles. The right-hand side highlights the different extent to which stacking surface is available for terminal pyrimidines and purines in the target strand.

of probes with a 5′-terminal purine residue by the same approach is more difficult because pyrimidines as terminal nucleobases in the target strand offer less surface area for stacking interactions than purines. Accordingly, the extent to which stacking on the terminus is bridging (and thus duplex stabilizing) is very limited. Here we present the results of a combinatorial search for molecular caps that enforce terminal A:T base pairs. The best acylamido substituent identified was developed into a phosphoramidite building block for automated DNA synthesis. The 5′-FEE was also combined with a FEE at the 2′-position of a modified 3′-terminal residue, generating doubly capped oligonucleotides that show increased mismatch discrimination at both termini.

## MATERIALS AND METHODS

### General information

The chemicals, instruments and general procedures were similar to those reported earlier (20) and are given in the Supplementary Material. Sequences are given from the 5′- to the 3′-terminus. In the term 'X:Y base pair', X represents the nucleotide of the probe strand and Y that of the target strand.

### DNA synthesis

The unmodified portion of oligodeoxynucleotides were prepared on a 1 μmol scale using a Perseptive Biosystems 8909 Expedite DNA synthesizer and the protocol provided by the manufacturer. Reaction columns for DNA synthesis were from Prime Synthesis (Aston, PA). Coupling reactions producing oligonucleotides with an aminopropanol phosphate linker at the 5′-terminus employed phosphoramidite **8** (23). The couplings of non-standard phosphoramidites **8**, **10**, **15** and **16** to solid-support-bound DNA used a 0.2 M solution (250 μl) of the respective phosphoramidite in $CH_2Cl_2$ or $CH_3CN$, the same volume of activator solution (4,5-dicyanoimidazole, 0.25 M in $CH_3CN$), and a reaction time of 30 min. These couplings were repeated once, followed by standard oxidation and deprotection. The extension with 5′-amino-5′-deoxynucleoside residues employed 35 mg solid support (~1 μmol oligonucleotide loading) and reaction cycles with the 3′-phosphoramidite building blocks of 5′-amino-2′,5′-deoxyadenosine (**1**) or 5′-amino-2′,5′-deoxythymidine (24,25) (200 μl of a 0.1 M solution in $CH_3CN$ for each), and reagents for a 1 μmol synthesis. The coupling time was extended to 200 s (instead of the 30 s used otherwise). The monomethoxytrityl group protecting the 5′-amine was removed by treating the support with Deblock Solution for DNA synthesizer (trichloroacetic acid–$CH_2Cl_2$, 3:97, 2 ml) for 2 min, followed by rinsing the support with $CH_2Cl_2$ (2× 2 ml) and drying (0.1 Torr).

### Synthesis of oligonucleotides with 5′-acylamido groups (General Protocol 1)

The following procedure for coupling of cholic acid to the cpg-bearing amino-terminal DNA **4** is representative. A mixture of HOBT (15.3 mg, 100 μmol), HBTU (34.1 mg, 90 μmol) and cholic acid (100 μmol) was dissolved in DMF (600 μl). Diisopropyl ethylamine (DIEA) (41 μl, 232 μmol) was added to this solution, followed by vortexing for 10 min. The resulting solution was added to the solid support displaying the amine (10 mg, ~0.25 μmol loading) in a polypropylene vessel. The slurry was slowly vortexed for 60 min. After removal of the supernatant, the solid support was washed with DMF (2× 1 ml) and $CH_3CN$ (2× 1 ml). The oligonucleotide was then deprotected and liberated from the support using General Protocol 3 (see below).

### Removal of Fmoc groups (General Protocol 2)

The Fmoc-protected modified oligonucleotide on controlled pore glass (10 mg, ~0.25 μmol loading) in a polypropylene reaction vessel was treated with piperidine in DMF (20%, 2 ml) for 20 min. The supernatant was aspired, and the solid support was washed with DMF (2 ml) and $CH_3CN$ (2× 1 ml), followed by drying at 0.1 Torr.

### Deprotection and cleavage from solid support (General Protocol 3)

After briefly drying *in vacuo*, the oligonucleotide-bearing cpg (20 mg, ~0.5 μmol loading) was treated with ammonium hydroxide (30% aqueous $NH_3$, 1 ml) in a polypropylene reaction vessel for 12 h at 25°C. Excess ammonia was then removed with a gentle air stream directed onto the surface of the solution for 60 min. The supernatant was aspired and the support washed with deionized water (2× 0.5 ml). The

combined solutions were filtered (0.2 µm pore size, Whatman Inc., Chilton, NJ) and either lyophilized or used directly for HPLC purification.

### 5′-*N*-Acetylation

The following protocol is for the synthesis of the solid-phase-bound precursor of **5a** and was used analogously for **6a.** The cpg-bound oligonucleotide (**4**) (10 mg, ~0.25 µmol loading) was treated with a mixture (2 ml, 1:1 v/v) of capping solution A for DNA synthesizers (acetic anhydride–2,6-lutidine–THF, 1:1:8 v/v) and capping solution B (1-methylimidazole–THF, 84:16 v/v) for 20 min, followed by rinsing with DMF (2× 2 ml) and $CH_3CN$ (2× 2 ml), and drying at 0.1 Torr. The oligonucleotide was then cleaved from the solid support using General Protocol 3.

### Oligonucleotide 5J

Using General Protocol 1, *N*-Fmoc-protected pipemidic acid (20) was activated on a 69 µmol scale and was coupled to amino-terminal DNA support **4** (10 mg, ~0.25 µmol loading). The removal of the Fmoc group was performed using General Protocol 2. Then, nalidixic acid was coupled to the oligonucleotide on the solid support, again using General Protocol 1 and 69 µmol of the acid. The title compound was liberated from the solid support using General Protocol 3.

### (*S*)-*N*-(Fluorenylmethoxycarbonyl)pyrrolidin-3-ol

A sample of (*S*)-3-pyrrolidinol (**11**) (200 mg, 2.3 mmol) was added to a suspension of an aqueous $NaHCO_3$ solution (10%, 6 ml) and 1,4-dioxane (6 ml) under stirring, followed by the addition of Fmoc-Cl (890 mg, 3.5 mmol). The resulting suspension was stirred for 18 h. The reaction mixture was then poured into saturated aqueous $NaHCO_3$ solution (25 ml) and extracted with $CH_2Cl_2$ (2× 25 ml). The combined organic phases were dried over $MgSO_4$ and reduced to dryness *in vacuo*. The resulting colorless oil was purified by column chromatography on silica with a step gradient of MeOH in $CH_2Cl_2$ (0–5%). The title compound was obtained as a colorless oil (0.69 g, 2.23 mmol, 84%). $R_f$ = 0.45 ($CH_2Cl_2$–MeOH, 95:5). $^1$H NMR ($CDCl_3$, 250 MHz) δ 1.85–1.99 (m, 2H), 3.45–3.56 (m, 4H), 4.18 (t, *J* = 6.7 Hz, 1H), 4.28–4.36 (m, 2H), 4.44 (br s, 1H), 7.20–7.37 (m, 4H), 7.54 (d, *J* =7.3 Hz, 2H), 7.70 (d, *J* = 7.3 Hz, 2H); HRMS (FAB, 3-NBA) calculated for $C_{19}H_{20}NO_3$ (M+H) 310.1443, found 310.1462.

### *O*-2-Cyanoethyl-*O*-[*N*-(fluorenylmethoxycarbonyl)-(*S*)-pyrrolidin-3-oxy]-(diisopropylamino)phosphoramidite (10)

A sample of *N*-Fmoc-protected pyrrolidinol (250 mg, 0.81 mmol), prepared as described in the preceding protocol, and diisopropylammonium tetrazolide (DIPAT) (70 mg, 0.4 mmol) in dry $CH_2Cl_2$ (2 ml) were treated with *O*-2-cyanoethyl-*N,N,N′,N′*-tetraisopropylphosphordiamidite (330 mg, 1.1 mmol). After complete conversion, the reaction mixture was poured into ethyl acetate (25 ml) and saturated aqueous $NaHCO_3$ solution (25 ml). The organic phase was washed twice with brine before being dried over $MgSO_4$, filtered and evaporated to dryness. The resulting oil was purified by column chromatography (silica, preconditioned with hexanes–$Et_3N$ 98:2), eluting with a step gradient of hexanes to hexanes–ethyl acetate 2:3. The title compound (mixture of diastereomers) was obtained as a colorless oil (0.37 g, 0.73 mmol, 89%). $R_f$ = 0.5 (hexanes–ethyl acetate 1:1). $^1$H NMR ($CDCl_3$, 250 MHz) δ 1.15–1.16 (m, 12H), 1.88–2.05 (m, 2H), 2.54 (q, *J* = 5.8 Hz, 2H), 3.43–3.56 (m, 6H), 3.64–3.80 (m, 2H), 4.13–4.22 (m, 1H), 4.26–4.34 (m, 1H), 4.40–4.49 (m, 1H), 7.19–7.36 (m, 4H), 7.54 (d, *J* = 7.3 Hz, 2H), 7.69 (d, *J* = 7.3 Hz, 2H).

### (*S*)-*N*-(1-Pyrenylmethyl)-pyrrolidin-3-ol

To a solution of (*S*)-3-pyrrolidinol (**11**) (135 mg, 1.5 mmol) and 1-pyrenecarboxaldehyde (350 mg, 1.5 mmol) in 1,2-dichloroethane (5 ml) was added sodium triacetoxyborohydride (647 mg, 3 mmol) in portions. The slurry cleared up in ~5 min. After 24 h, aqueous $NaHCO_3$ (20 ml, 5%) was added, and the aqueous phase was back-extracted with ethyl acetate (3× 20 ml). The combined organic phases were dried over $Na_2SO_4$ and the solvent was removed *in vacuo*. Chromatography on silica with $CH_2Cl_2$–MeOH (9:1) yielded 422 mg (1.4 mmol, 93%) of the title compound as a yellow oil. $R_f$ = 0.45 ($CH_2Cl_2$–MeOH, 9:1). $^1$H-NMR ($CDCl_3$, 250 MHz) δ 1.46–1.61 (m, 1H), 1.89–2.05 (m, 1H), 2.16–2.29 (m, 1H), 2.37–2.46 (m, 1H), 2.50–2.58 (m, 1H), 2.66–2.80 (m, 2H), 4.09 (s, 2H), 7.75–8.01 (m, 9H), 8.27 (d, *J* = 9.2 Hz, 2H); MALDI-TOF MS (ATT): 300 ($M^+$), 215 ($C_{16}H_9$-$CH_2^+$). The (*R*)-isomer of the title compound was prepared analogously, starting from **17**.

### *O*-2-Cyanoethyl-*N,N*-diisopropyl-*O*-[*N*-(1-pyrenylmethyl)-(*S*)-pyrrolidin-3-oxy]-phosphoramidite (16)

To a solution of pyrenylmethylpyrrolidinol (400 mg, 1.32 mmol) and DIEA (700 µl, 1.21 mmol) in anhydrous $CH_3CN$ (5 ml) was added 2-cyanoethyl-*N,N*-diisopropyl-chlorophosphoramidite (400 µl, 1.83 mmol). After full conversion of the starting material (3 h), ethyl acetate (20 ml) was added, and the solution was washed with a saturated aqueous solution of $NaHCO_3$ (2× 20 ml) and with brine (2× 20 ml). The organic phase was dried over $Na_2SO_4$ and the solvent was removed *in vacuo.* Chromatography on silica (50 g) with cyclohexane–acetone (3:2) containing 1% $NEt_3$ gave 542 mg (1.08 mmol, 82%) of **16** as a yellow oil. $^{31}$P-NMR ($CDCl_3$–$NEt_3$, 202 MHz) δ 137.3. The (*R*)-isomer of the title compound (**15**) was prepared analogously.

### Oligonucleotides with 3′-terminal 2′-(anthraquinon-2-yl-carboxamido)-2′-deoxyuridine residues

The solid support with the 2′-acylamido-2′-deoxyuridine residue (**18**) (11 mg, ~0.5 µmol loading) was prepared as detailed in the Supplementary Material. All further steps were performed analogously to those described above.

### Analytical data

The analytical data given for **14**, below, are representative for the oligonucleotides that were HPLC purified. A full list of the data for the other compounds can be found in the Supplementary Material.

Ω-*AGGTTGAC* (**14**). Yield: 42%. HPLC: $CH_3CN$ gradient, 0% for 5 min to 25% in 45 min, $t_R$ = 40 min. MALDI-TOF MS for $C_{100}H_{116}N_{33}O_{49}P_8$ $[M-H]^-$: calculated 2812.0, found 2813.0.

### UV melting experiments

UV melting experiments were essentially performed as reported earlier (20). Details are given in the Supplementary Material.

## RESULTS

The first phase of the current study focused on identifying affinity- and fidelity-enhancing caps from the large structure space of commercially available carboxylic acids. These were attached to the 5′-terminal deoxyadenosine residue through a direct peptidic link to avoid the entropic cost of folding a flexible linker when forming a capped duplex. This required the synthesis of a suitably protected 5′-amino-2′-5′-dideoxyadenosine phosphoramidite. The synthetic route of Mag and Engels (26) to **1** (Scheme 1) was slightly modified. Specifically, a more regioselective tosylation was achieved by using 1.5 equivalents of tosyl chloride, and sodium azide was employed in the subsequent step instead of lithium azide. Standard DNA synthesis starting from support **2** provided heptamer **3**, which was extended to **4** using **1**. Support-bound amine **4** was derivatized with carboxylic acid residues by activating the acids with HBTU/HOBT in the presence of Hünig's base and adding the acylation mixture to the solid support. Deprotection with aqueous ammonia at room temperature gave 5′-acylamido octamers of general structure **5**. Sets of five to six of these compounds were pooled into libraries (chemsets), which were subjected to spectrometrically monitored selection experiments (SMOSE) (27). The spectra of the chemsets are shown in the Supplementary Material. For the selection, solutions of the mixtures spiked with one equivalent of target strand 5′-GTCAACCT-3′ were treated with snake venom phosphodiesterase, which digests unbound strands from the 3′-terminus. Oligonucleotides with 5′-caps that stabilize the duplex with the target strand to the greatest extent survive the longest under these conditions and can be identified via MALDI-TOF mass spectrometry (20,22). Every library contained **5a** as reference compound, and integration of degradation kinetics allowed the calculation of protection factors relative to **5a**, as described previously for assays leading to caps for oligonucleotides with 5′-terminal pyrimidines (22).

The lower part of Scheme 1 shows the acylamido caps tested via nuclease selection, together with the protection factors obtained for the oligonucleotides carrying them. While small substituents had no noticeable effect on nuclease survival, many of the aromatic bicyclic and tricyclic residues gave protection factors between 1 and 1.6. This included quinolones, i.e. hits identified in selections where the acyl groups were appended to 5′-terminal pyrimidines (20,22). The cholic acid residue (**M**), another moiety that came up as a hit in selections involving oligonucleotides with 5′-pyrimidine residues (20,22), gave a protection factor above 1.6, but the highest protection factor was measured for the oligonucleotide displaying the residue of pyrene butyric acid (**r**).

Interestingly, the residue of pyrene carboxylic acid (**l**), which lacks the flexible propylene linker of substituent **r**, did not appear to stabilize the duplex perceptibly, as evidenced by the low protection factor of 1.1. This prompted us to synthesize an oligonucleotide where the pyrene butyric acid residue is appended to the 5′-terminus via an aminopropanol phosphate linker [general structure **6** (Scheme 2)]. The oligonucleotide was prepared by extending solid-support-bound **7** via a coupling cycle with phosphoramidite **8** (23) and acylating under peptide coupling conditions, as described above. The linker–cap moieties could, in principle, have been introduced via automated DNA synthesis, if linker and acyl group had been coupled separately and the resulting amide been phosphitylated, but the combinatorial synthesis of all derivatives from a common solid-support-bound precursor required less synthetic effort. Unfortunately, oligonucleotides **6k**, **6s**, **6m** and **6r** all gave a lower protection factor than **5r**, so that the design based on an aminopropanol phosphate linker was not pursued further.

Instead, the linker between the acyl group and the 5′-terminus of the oligonucleotide was changed to a pyrrolidine phosphate group, i.e. a linker that is more rigid but retains the phosphodiester linkage that allows for the generation of phosphoramidite building blocks. The pyrrolidine phosphate moiety was also believed to mimic the deoxyribose phosphate backbone of natural DNA and thus pre-orient the acyl residue toward stacking on the terminal base pair. Oligonucleotides of general structure **9** were prepared, as detailed in Scheme 3. The phosphoramidite of the pyrrolidine linker (**10**) was prepared from the (*S*)-enantiomer of 3-hydroxypyrrolidine (**11**) by Fmoc-protection of the secondary amine and phosphitylation of the hydroxyl group. Compound **10** was employed in a DNA extension cycle, producing **12**, whose direct deprotection gave **9Q**. On-support coupling to selected carboxylic acids followed by deprotection gave target compounds **9m**, **9M**, **9n**, **9K**, **9L**, **9s**, **9X**, **9Y** and **9Z**. The oligonucleotides with non-pyrenyl caps were again tested in MALDI-monitored nuclease selections, but did not yield any new hit. Pyrene-bearing oligonucleotides **9X**, **9Y** and **9Z**, which are derivatives of lead compound **5r**, were purified and directly subjected to UV melting analyses. The duplex between pyrene butyric acid-bearing **9X** and its target strand gave a higher melting point than its counterpart **5r** with a directly appended pyrene butyric acid (Table 1). Neither of the oligonucleotides displaying pyrene carboxylic acid or its nitro derivative via the pyrrolidine linker (**9Z**, **9Y**) gave a higher melting point than **9X** (Table 1).

Next, pyrenylmethyl-substituted oligonucleotides **13** and **14** were prepared (Scheme 4). These were believed to have the advantage of a more flexible linker between the hydroxypyrrolidine ring and the pyrene moiety, because the rotation of the bond between the nitrogen atom of the pyrrolidine ring and the pyrenyl ring system is not restricted by an amide resonance. Also, their tertiary amino group may be protonated at physiological pH, favoring duplex formation electrostatically. Further, phosphoramidites **15** and **16** could be readily prepared in two steps from inexpensive starting materials **11**/**17** and pyrene carboxaldehyde, avoiding the lengthy and low yielding synthesis of a *C*-nucleoside. The synthesis of the phosphoramidites proceeded uneventfully, with pyrene carboxaldehyde undergoing reductive amination with **11** or **17** in 1,2-dichloroethane, and the resulting alcohols were phosphitylated under standard conditions to give **15** and **16**. Oligonucleotides with pyrenylmethyl moiety show characteristic fragmentation

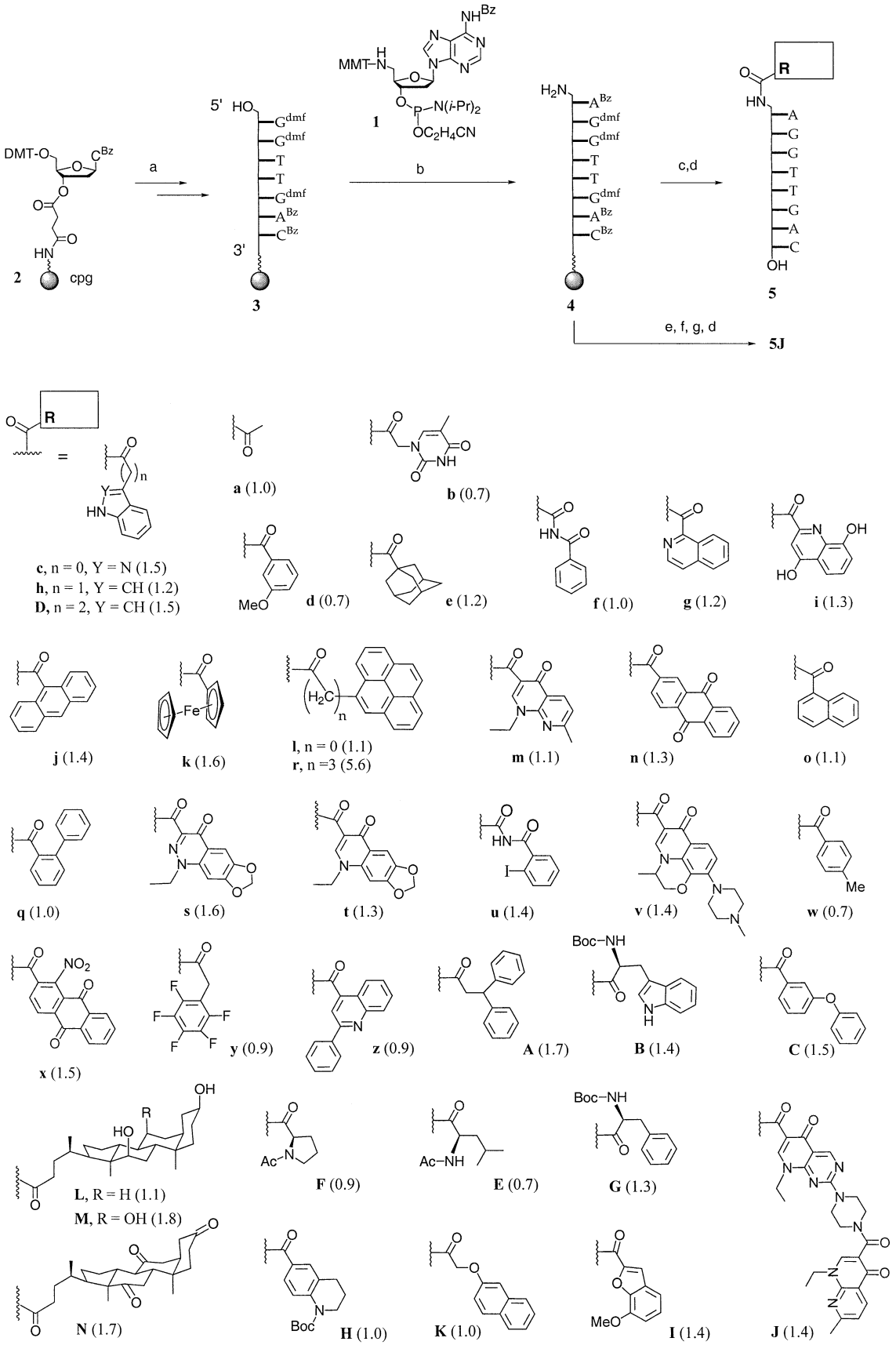


**Scheme 1.** (a) Standard DNA synthesis; (b) extension cycle with **1**; (c) R-$CO_2H$, HBTU, HOBT, DIEA, DMF; (d) $NH_4OH$; (e) Fmoc-pipemidic acid, HBTU, HOBT, DIEA, DMF; (f) piperidine, DMF; (g) nalidixic acid, HBTU, HOBT, DIEA, DMF. Numbers in parentheses are protection factors measured for the respective derivatives of **5** in nuclease selection assays (22).

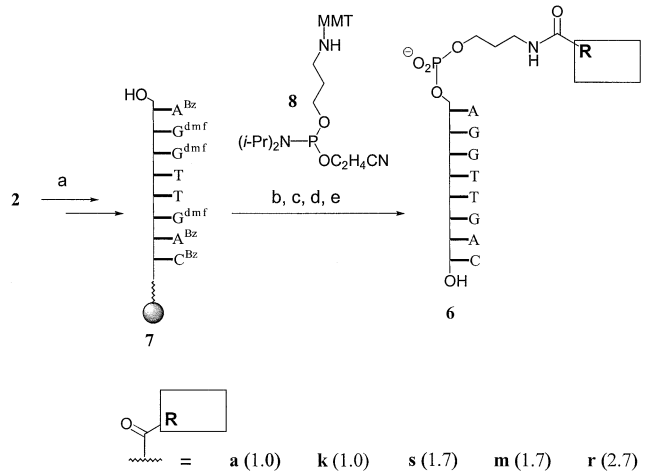

**Scheme 2.** (a) Standard DNA synthesis; (b) extension cycle with **8**; (c) trichloroacetic acid, $CH_2Cl_2$; (d) R-$CO_2H$, HBTU, HOBT, DIEA, DMF; (e) $NH_4OH$.

**Table 1.** UV melting results for octamers and target strand 5′-GTCAACCT-3′

| Probe | Melting point (°C)[a] [salt] = 150 mM | [salt] = 1 M | ΔTm 1 M (°C)[b] | Hyperchromicity 1 M (%)[c] |
|---|---|---|---|---|
| AGGTTGAC | 31.5 ± 0.8 | 35.9 ± 0.6 | – | 18.2 |
| **5a** | 31.5 ± 0.8 | 34.5 ± 0.8 | – | 6.2 |
| **5r** | 39.7 ± 0.8 | 43.7 ± 0.2 | +9.2 | 16.3 |
| **5s** | 38.9 ± 0.6 | 43.4 ± 0.7 | +8.9 | 9.8 |
| **5J** | 36.2 ± 1.6 | 38.3 ± 1.6 | +3.8 | 8.3 |
| **5L** | 38.9 ± 0.6 | 43.2 ± 0.6 | +8.7 | 13.2 |
| **5M** | 39.5 ± 0.9 | 43.6 ± 0.9 | +9.1 | 16.7 |
| **5N** | 33.2 ± 0.8 | 37.8 ± 0.8 | +3.3 | 6.8 |
| **9n** | 37.0 ± 0.7 | 43.8 ± 0.7 | +9.3 | 17.1 |
| **9m** | 36.4 ± 0.9 | 43.0 ± 0.7 | +8.5 | 21.5 |
| **9X** | 37.8 ± 0.6 | 44.5 ± 0.2 | +10.0 | 24.1 |
| **9Y** | 35.5 ± 0.8 | 42.1 ± 0.8 | +7.6 | 19.4 |
| **9Z** | 35.2 ± 0.7 | 41.9 ± 0.5 | +7.4 | 20.7 |
| **14** | 39.3 ± 0.4 | 45.4 ± 0.2 | +10.9 | 23.7 |
| **13** | 39.1 ± 1.8 | 43.9 ± 1.2 | +9.4 | 17.9 |

[a]Average of four melting points ± SD at 2.5 μM strand concentration at the respective $NH_4OAc$ concentration.
[b]Melting point difference to control duplex (AGGTTGAC:GTCAACCT) at 1 M $NH_4OAc$.
[c]Hyperchromicity upon duplex dissociation at 1 M $NH_4OAc$.

in the MALDI mass spectrum, with prominent peaks for both the pseudomolecular ion and the fragment resulting from 'benzylic' cleavage (see spectra in the Supplementary Material).

Gratifyingly, the duplexes of **13** and **14** gave higher melting points than any of the caps tested (Table 1) although, interestingly, the isomer with the (*S*)-configured pyrrolidine linker (**14**), which presumably mimics the stereochemical configuration of the deoxynucleoside less closely, gave a higher $\Delta T_m$ (+10.9°C at 1 M salt). At the same time, the capping of the duplex did not reduce the cooperativity of the melting transition (Fig. 2), as one might have feared when stabilizing only one terminus of a duplex. In fact, the half-height width of the peak that duplex dissociation causes in the first derivative of the melting curve is 18.0°C for the control duplex AGGTTGAC:GTCAACCT and 16.4°C for **14:**GTCAACCT at 1 M salt and 2.5 μM strand concentration. When the melting points of duplexes between **14** and target strands with a mismatched nucleobase were measured, the desired effect of pyrenylmethylpyrrolidine phosphate of increasing base-pairing fidelity was observed. Melting point decreases over the fully matched duplex of 6.3–8.3°C for a terminal mismatch and 14.1–16.2°C for a mismatch at the penultimate position of the duplex were found, which are considerably greater than those of the control duplexes lacking the cap (Table 2).

We then wished to find a cap that can be combined with the optimized 5′-cap and may be appended to the 3′-terminal residue of longer oligonucleotides, generating doubly capped hybridization probes. The residue of anthraquinone carboxylic acid (n) has recently been shown to stabilize duplexes when appended to the 2′-position of a 2′-deoxyuridine residue at the 3′-terminus (28). We therefore studied the base-pairing tolerance of duplexes formed by octamer 5′-AGGTTGA(U-**n**)/T-3′, where the 3′-terminal residue is either the modified deoxyuridine residue or a thymidine residue. The synthesis of the modified oligonucleotide started from solid support **18**, shown in Scheme 5. The melting points of the duplexes with a single mismatch at the terminal or penultimate position dropped more sharply for the duplexes with the 2′-cap than for those that lacked it (Table 3), demonstrating that the

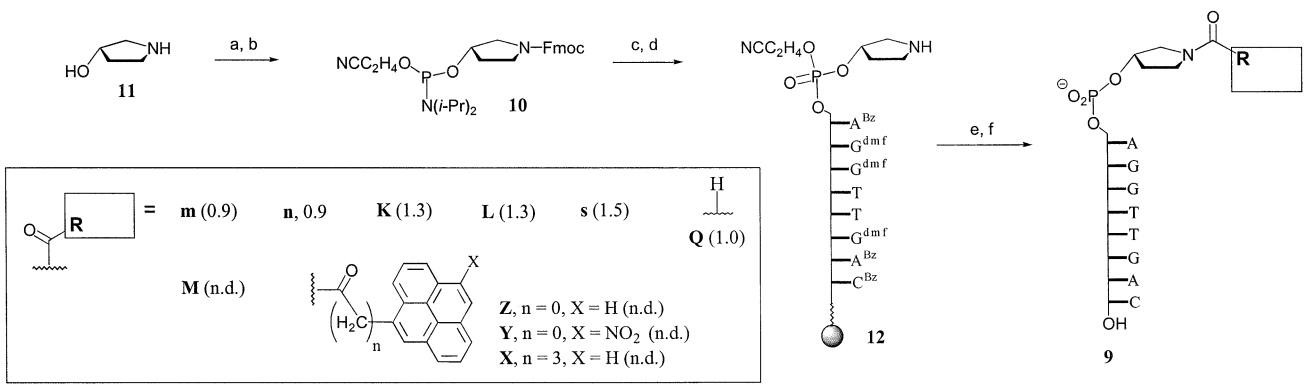

**Scheme 3.** (a) Fmoc-Cl, $NaHCO_3$, dioxane, water (84%); (b) $P(OC_2H_4CN)(NiPr_2)_2$, DIPAT, $CH_3CN$ (89%); (c) extension cycle with **10**; (d) piperidine, DMF; (e) R-$CO_2H$, HBTU, HOBT, DIEA, DMF; (f) $NH_4OH$.

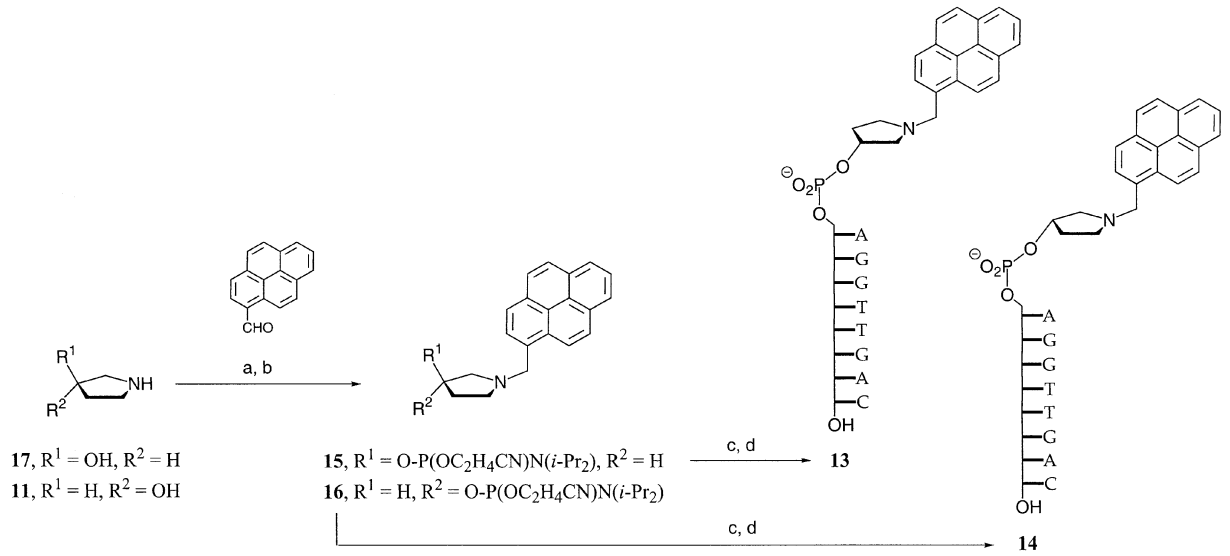


**Scheme 4.** (a) $NaBH(OAc)_3$, 1,2-dichloroethane; (93%); (b) $ClP(OC_2H_4CN)NiPr_2$, DIEA, $CH_3CN$ (82%); (c) extension cycle with **15** or **16**; (d) $NH_4OH$.

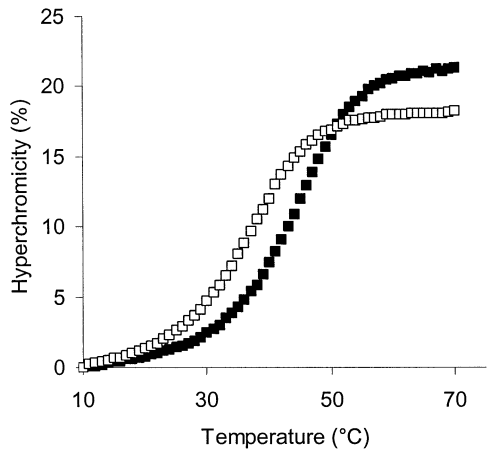


**Figure 2.** UV melting curves of oligonucleotide duplexes at 2.5 μM strand concentration, 1 M ammonium acetate buffer pH 7: open squares, control duplex AGGTTGAC:GTCAACCT; filled squares, **14:**GTCAACCT**.**

**Table 2.** UV melting points of octamer duplexes containing single mismatches at or next to the 5′-terminus

| Probe | Target sequence | Mismatch | $T_m$[a] (°C) | $\Delta T_m$[b] (°C) |
|---|---|---|---|---|
| AGGTTGAC | GTCAACCA | A:A | 32.7[c] | –2.2 |
| **14** | GTCAACCA | A:A | 37.5 ± 1.3 | –8.3 |
| **5r** | GTCAACCA | A:A | 36.2 ± 0.6 | –7.5 |
| **5M** | GTCAACCA | A:A | 37.9[c] | –5.7 |
| AGGTTGAC | GTCAACCC | A:C | 33.7[c] | –1.2 |
| **14** | GTCAACCC | A:C | 39.6 ± 0.6 | –6.6 |
| **5r** | GTCAACCC | A:C | 36.3 ± 0.6 | –7.4 |
| **5M** | GTCAACCC | A:C | 37.5[c] | –6.1 |
| AGGTTGAC | GTCAACCG | A:G | 33.8[c] | –1.1 |
| **14** | GTCAACCG | A:G | 39.5 ± 1.3 | –6.3 |
| **5r** | GTCAACCG | A:G | 37.4 ± 0.4 | –6.3 |
| **5M** | GTCAACCG | A:G | 39.2[c] | –4.4 |
| AGGTTGAC | GTCAACAA | G:A | 23.1 ± 0.8 | –12.8 |
| **14** | GTCAACAA | G:A | 29.6 ± 1.2 | –16.2 |
| AGGTTGAC | GTCAACGA | G:G | 23.6 ± 1.0 | –12.3 |
| **14** | GTCAACGA | G:G | 32.0 ± 0.9 | –13.8 |
| AGGTTGAC | GTCAACTA | G:T | 24.4 ± 1.0 | –11.5 |
| **14** | GTCAACTA | G:T | 31.6 ± 0.9 | –14.1 |

[a]Average of four melting points ± SD at 1.5 μM strand concentration and 1 M $NH_4OAc$.
[b]Melting point difference from fully complementary duplex.
[c]SD not determined.

acylamido substituent improved the mismatch discrimination in every case. This was not a trivial result, since studies with 5′-appended quinolones, structurally related to anthraquinone carboxylic acid, show that such residues can also interact by disrupting the terminal base pair (29).

Next, we used the fidelity-enhancing caps together, generating oligonucleotides **19** and **20**, which contain a capped 5′-terminal deoxyadenosine residue and a capped 3′-terminal 2′-acylamido-2′-deoxyuridine residue (Scheme 5). The strand with the 5′-terminal thymidine residue (**20**) was prepared because its sequence has been tested extensively with other modified residues (30). Anthraquinone-bearing solid support **18** was extended to **21** or **22** via automated DNA synthesis, followed by coupling with **16** and deprotection to generate **19** and **20**. Additionally, extension of **18** to a dodecamer using the phosphoramidite building block of 5′-amino-5′-deoxythymidine (24,25) in the last extension cycle gave **23**. Acylation with pyrene butyric acid and deprotection led to **24**, which allowed for a comparison of the two pyrenyl caps Ω and Ψ on the level of dodecamers. The UV melting points of the duplexes of the doubly capped oligonucleotides and their fully complementary target strands, as well as those of the unmodified control duplexes, are compiled in Table 4. As expected, the melting point increase over the unmodified duplexes was less for the longer sequence than for the octamers. The bridging effect of the cap was greater for **20**

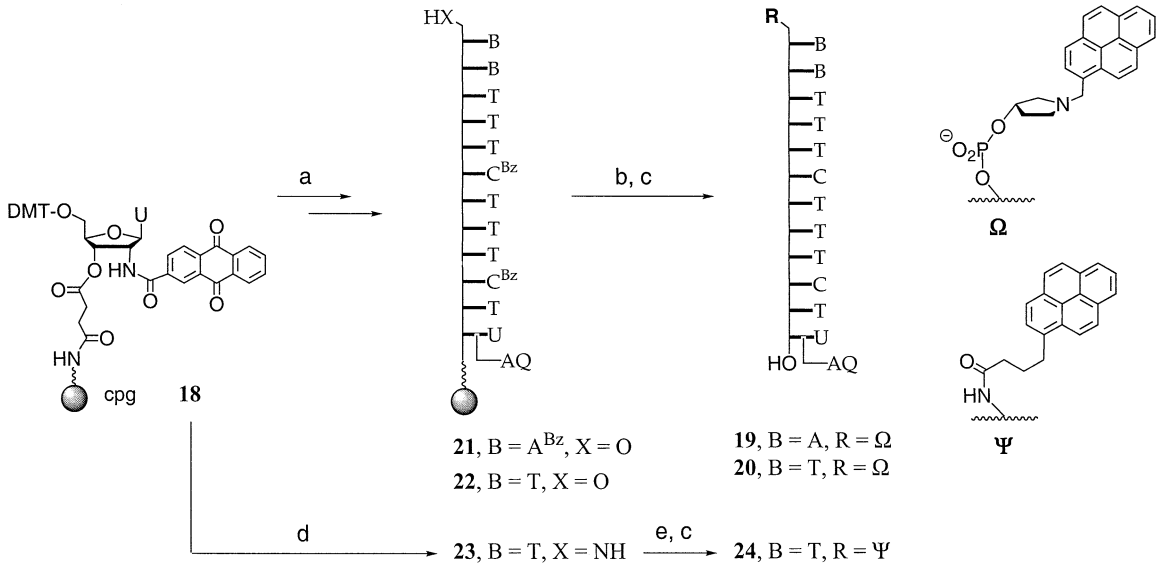


**Scheme 5.** (a) Standard DNA synthesis; (b) extension cycle with **16**; (c) $NH_4OH$; (d) DNA synthesis with coupling of the phosphoramidite building block of 5′-amino-5′-deoxythymidine in the last extension cycle; (e) pyren-1-yl-butyric acid, HBTU, HOBT, DIEA, DMF.

**Table 3.** UV melting points of octamer duplexes with mismatches at the 3′-terminus

| Probe | Target sequence | Mismatch | $T_m$[a] (°C) [salt] = 150 mM | [salt] = 1 M | $\Delta T_m$ 1 M[b] (°C) |
|---|---|---|---|---|---|
| AGGTTGAT | **C**TCAACCT | T:C | 18.2 ± 0.5 | 23.9 ± 0.5 | –2.4 |
| AGGTTGAU-**n** (**25**) | **C**TCAACCT | U:C | 30.0 ± 0.9 | 36.9 ± 0.8 | –3.8 |
| AGGTTGAT | **G**TCAACCT | T:G | 19.6 ± 0.8 | 25.1 ± 1.0 | –1.2 |
| AGGTTGAU-**n** (**25**) | **G**TCAACCT | U:G | 30.0 ± 0.9 | 38.9 ± 0.5 | –1.7 |
| AGGTTGAT | **T**TCAACCT | T:T | 20.3 ± 1.0 | 25.9 ± 1.0 | –0.4 |
| AGGTTGAU-**n** (**25**) | **T**TCAACCT | U:T | 30.7 ± 1.0 | 35.9 ± 1.0 | –4.8 |
| AGGTTGAT | A**A**CAACCT | A:A | <15 | 21.6 ± 1.2 | –4.7 |
| AGGTTGAU-**n** (**25**) | A**A**CAACCT | A:A | 23.5 ± 1.3 | 31.2 ± 1.2 | –9.5 |
| AGGTTGAT | A**C**CAACCT | A:C | <15 | 19.1 ± 0.4 | –7.2 |
| AGGTTGAU-**n** (**25**) | A**C**CAACCT | A:C | 18.3 ± 0.4 | 25.8 ± 1.0 | –14.9 |
| AGGTTGAT | A**G**CAACCT | A:G | <15 | <15 | – |
| AGGTTGAU-**n** (**25**) | A**G**CAACCT | A:G | <15 | 15.9 ± 0.4 | –24.4 |

[a]Average of four melting points ± SD at 1.5 μM strand concentration and $NH_4OAc$.
[b]Melting point difference from fully complementary strand at 1M $NH_4OAc$.

than for **19**, since the latter features a purine base at its 5′-terminus. Still, $\Delta T_m$ values of more than +10°C were measured even in the most unfavorable case. Further, cap Ω was more duplex-stabilizing than Ψ, confirming the results of the optimization study performed on the octamer level. A duplex of doubly capped **20** and an octadecamer target strand that carries overhangs at both termini also gave a $\Delta T_m$ of >+10°C at both salt concentrations tested (entries 6 and 7 of Table 4), indicating that blunt ends are not required for the caps to exhibit their duplex-stabilizing effect.

Table 5 shows the results from an exploratory UV melting study on mismatch discrimination involving doubly capped **19** and **20** and their unmodified counterparts. Target strands with mismatches at both the 3′- and 5′-termini led to melting point decreases of no more than 0.3–1.7°C for the unmodified control dodecamers. Doubly capped **19** and **20**, on the other hand, gave melting point decreases of 6.2–7.4°C, confirming the fidelity-enhancing effect of the caps. Even with mismatches at the two penultimate positions of the target strand, a substantial fidelity increase was observed for **20** compared with the unmodified dodecamer.

## DISCUSSION

Of the two weak terminal base pairs that mispair particularly easily, namely the T:A and the A:T base pair, the A:T base pair should be the most error prone. The contact area between the remainder of the duplex and the 3′-terminal nucleobase of the target strand is smaller for a pyrimidine than for a purine in the target (Fig. 1). If similar hydrogen-bonding strengths and similar stacking forces per square Angstrom are involved, this should mean fewer interactions on which discrimination can be based for the case where the pyrimidine is the target base. A comparison of the melting point depressions caused by the

**Table 4.** UV melting points and hyperchromicities of dodecamer duplexes

| Probe | Target sequence | $T_m$[a] (°C) [salt] = 100 mM | [salt] = 1 M | $\Delta T_m$ 1 M[b] (°C) | Hyperchromicity[c] (%) |
|---|---|---|---|---|---|
| AATTTCTTTCTT | AAGAAAGAAATT | 38.4 ± 0.3 | 42.1 ± 0.6 | – | 30.9 ± 0.2 |
| **19** | AAGAAAGAAATT | 48.4 ± 0.6 | 53.2 ± 0.5 | +11.1 | 22.6 ± 0.2 |
| TTTTTCTTTCTT | AAGAAAGAAAAA | 35.6 ± 0.9 | 37.3 ± 0.9 | – | 30.4 ± 0.5 |
| **20** | AAGAAAGAAAAA | 47.7 ± 0.3 | 52.9 ± 0.3 | +15.6 | 29.3 ± 1.2 |
| **24** | AAGAAAGAAAAA | 45.0 ± 0.9 | 46.3 ± 0.9 | +9.0 | 26.1 ± 1.1 |
| TTTTTCTTTCTT | CGAAAGAAAGAAAAAAGC | 38.2 ± 0.2 | 42.1 ± 0.4 | – | 26.2 ± 0.8 |
| **20** | CGAAAGAAAGAAAAAAGC | 48.7 ± 0.3 | 53.7 ± 0.4 | +11.6 | 30.9 ± 1.5 |

[a]Average of four melting points ± SD at 1.6 μM strand concentration and 10 mM PIPES buffer, 10 mM $MgCl_2$ and NaCl concentration given.
[b]Melting point difference to fully complementary duplex.
[c]Hyperchromicity upon duplex dissociation at 260 nm.

**Table 5.** UV melting points of dodecamer duplexes containing two mismatches at or next to the terminus[a]

| Probe | Target sequence | Mismatches | $T_m$[b] (°C) | $\Delta T_m$[c] (°C) |
|---|---|---|---|---|
| AATTTCTTTCTT | **T**AGAAAGAAAT**A** | A:A, T:T | 40.4 ± 1.1 | –1.7 |
| **19** | **T**AGAAAGAAAT**A** | A:A, U:T | 45.8 ± 0.6 | –7.4 |
| TTTTTCTTTCTT | **T**AGAAAGAAAA**T** | T:T, T:T | 36.8 ± 0.4 | –0.3 |
| **20** | **T**AGAAAGAAAA**T** | T:T, U:T | 46.7 ± 0.4 | –6.2 |
| TTTTTCTTTCTT | A**C**GAAAGAAA**C**A | T:C, T:C | 28.4 ± 0.4 | –8.8 |
| **20** | A**C**GAAAGAAA**C**A | T:C, T:C | 40.4 ± 0.4 | –12.5 |

[a]Buffer conditions: 10 mM PIPES, 10 mM $MgCl_2$, 1 M NaCl.
[b]Average of four melting points ± SD at 1.6 μM strand concentration.
[c]Melting point difference to fully complementary duplex.

three possible terminal mismatches for the duplexes of 5′-NGGTTGAC-3′, with N being A, T or C, shows that the 5′-terminal deoxyadenosine does indeed give the lowest fidelity. For N = T, the mismatches cause $\Delta T_m$ values of between –1.9 and –2.5°C (8), for N = C, values between –4.9 and –6.6°C are measured (20), whereas N = A gives values between –1.1 and –2.2°C (Table 2). Besides the differences between pyrimidines and purines as target bases, these numbers also show how much more selective the stronger C:G base pair is than the T:A and A:T base pairs. This confirms the need to enforce the weak base pairs to achieve high-fidelity recognition.

It is interesting that the pyrene butyric acid residue (**r**) was also tested as a molecular cap in an earlier study where it was attached to a deoxyuridine residue (28), but did not come up as a hit in the nuclease selection. In the present study, where the residue carrying the cap was deoxyadenosine, pyrene butyric acid gave both the highest protection factor and the greatest melting point increase among the 5′-acylamido groups tested. This may be due to the different nucleobases at the terminus of the target strand. If this nucleobase is long and narrow, a cap that is long and narrow should fit best. For adenine as target base, this seems to be the case for the residues of cholic acid (21) and anthraquinone carboxylic acid (28) when appended at the 5′- or the 2′-position, respectively. When the target nucleobase is short and wide, as is the case with thymine with its monocyclic structure and extrahelical methyl group, a cap that is wide enough to cover it entirely is apparently required to achieve a strong bridging effect. Hence the pyrenyl group is an 'expected' hit in the current study. To reach the thymidine in the target strand, the pyrenyl ring system must be attached to the probe strand via a linker of sufficient length, which might explain why pyrene carboxylic acid (**l**) is less effective than **r** or Ω. In the optimized cap Ω, the hyroxypyrrolidine ring that mimics the deoxyribose of the related *C*-nucleoside (30–32) may preorient the pyrenyl group by packing against the deoxyadenosine residue. If its tertiary amine is protonated, a small favorable electrostatic contribution for duplex stability may also result. The methylene spacer between the nitrogen atom of the pyrrolidine ring and the pyrenyl ring system may keep the latter 'in position' for stacking on the T, since pyrene is a little smaller than a base pair (31).

The stacking between the aromatic portion of the cap and the nucleobase in the target strand may also benefit from a donor–acceptor situation. The pyrene ring is electron rich and it may stack favorably on the electron-deficient thymine ring. In the case of the anthraquinoyl group (n) attached to the 2′-position of the 3′-terminal deoxyuridine residue (**25**, Table 3), the aromatic ring is electron deficient and therefore may stack well on the electron-rich adenine at the 5′-terminus of the target strand. The melting point increase of up to 14°C per residue induced by the 2′-cap when bridging a hexamer (28) is the strongest measured to date in our work.

Further, it was unexpected that the (*S*)- rather than the (*R*)-isomer of the pyrrolidine-containing cap provides the greater duplex-stabilizing effect, as determined via UV melting analysis. The structural similarity between the (*R*)-enantiomer of the *N*-methylpyrrolidine phosphate residue and the backbone of a deoxynucleoside may have suggested otherwise (Fig. 3). However, as the representation of the (*S*)-hydroxypyrrolidine residue in Figure 3 shows, the difference in overall structure is small between the isomeric linkages, and an arrangement of the linker similar to that of deoxyriboses in DNA duplexes is possible for both.

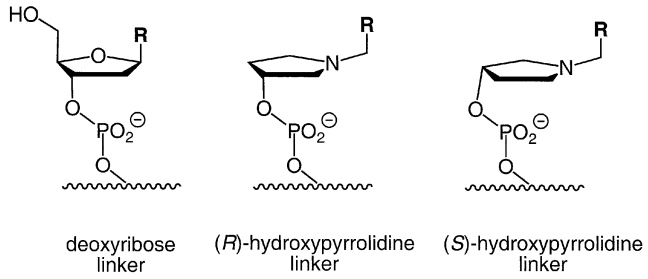


**Figure 3.** Structure of the linker portions of dangling residues with regular DNA backbone (left) or hydroxypyrrolidine backbone of either stereochemical configuration (middle and right): R, nucleobase or base surrogate acting as a molecular cap.

It is also interesting to compare the duplex-stabilizing effect of the pyrenylmethylpyrrolidine phosphate cap Ω with that of the pyrenyl *C*-nucleoside. The latter, when employed as 5′-dangling residue of the self-complementary hexamer $(CGCGCG)_2$, gives a melting point increase of 11.55°C per cap (30,32). For our cap Ω, when 5′-appended to AGGTTGAC, the value is +10.9°C. This may seem marginally lower, but it must be borne in mind that the ΔTm is being measured on a longer duplex, where the effect of individual residues on total duplex stability is smaller, and with a 5′-terminal purine rather than pyrimidine residue, where the bridging effect is smaller (compare the melting points for **19** and **20** in Table 4). It is known from modified (33) and unmodified (34) sequences that very short duplexes can give strong effects for dangling residues. The synthesis of the phosphoramidite of the *C*-nucleoside, starting from 2-deoxyribose and 1-bromopyrene, is at least seven steps, not counting the generation of the Grignard reagent plus transmetallation and the epimerization step (35). It involves organocadmium compounds and the separation of anomers. The synthesis of **16** from commercially available compounds consists of only two high yielding steps, making it an attractive alternative.

In this context, it is also worth discussing to what extent the changes in duplex stability upon introducing dangling *C*-nucleotides are measurements of total 'aromatic stacking affinities' of the dangling bases (32). Probably, gains in duplex stability are the result of several factors, including direct stacking interactions, strengthening of hydrogen bonds that are being shielded from solvent and hydrophobic effects. Perhaps more importantly, the change in the free energy of duplex formation reflects only the portion of the interactions that are bridging the duplex. The (substantial) portion of stacking interactions that occurs *intra*strand, i.e. between the dangling residue and the terminal residue to which it is appended, may not increase duplex stability.

Next, it is worthwhile discussing the possible structural basis for the increase in base-pairing fidelity caused by the pyrenylmethylpyrrolidine cap (Ω). The melting points (Tables 2 and 5) show that duplexes with mismatched terminal base pairs do not experience the same duplex-stabilizing effect as those with canonical A:T or T:A base pairs. Given the size of the pyrene ring system (36), purine:purine base pairs are probably too large to be fully covered by the cap, whereas pyrimidine:pyrimidine pairs may be too small to accommodate it (the plane of the base pair is delimited by the deoxyribose rings). Further, since the pyrenyl group shields the terminal base pair from water and thus increases the stability of hydrogen bonds, intrinsically stronger canonical hydrogen bonds may be stabilized more than those of competing mismatched base pairs. Similar arguments hold for the residue of anthraquinone carboxylic acid appended to the 2′-position of the 3′-terminal aminodeoxyuridine residue. Here, however, the base-pairing fidelity is even lower for the control duplex, with a melting point depression as low as –0.4°C for a T:T pair (Table 3). Also, T/U:G wobble base pairs remain difficult to resolve from T/U:A base pairs, even with the anthraquinone cap. The reduced effect of a cap at the 3′-terminus is similar to the small duplex-stabilizing effect of dangling residues at the 3′-terminus of DNA duplexes, compared with the same residues at the 5′-terminus (37). We believe there is room for improvement of FEEs at the 3′-terminal residue.

Nevertheless, the enhanced affinity and base-pairing fidelity of the doubly capped oligonucleotides described here constitute a step towards high-fidelity hybridization probes. The result for the pyrenylmethylpyrrolidine phosphate cap Ω with dodecamers **19** and **20**, which feature 5′-terminal deoxyadenosine and thymidine residue, suggests that this cap can be used for each of the weakly pairing nucleosides at the 5′-terminus, making the need for customized caps for either residue unwarranted. If a readily accessible and versatile set of FEEs can be developed that increase base-pairing fidelity at the termini and adjust the stability of A/T- and G/C-rich sequences, high-fidelity hybridization on a genome-wide level should become easier. Increased base-pairing fidelity has been demonstrated for 5′-capped probes on microarrays (38). The advantage of non-nucleosidic FEEs over other strategies, such as introducing artificial mismatches (39) or lengthening the probe, is that they are orthogonal in their binding properties, meaning that they do not offer additional binding sites for related sequences and thus do not encourage cross-hybridization.

## SUPPLEMENTARY MATERIAL

Supplementary Material is available at NAR Online.

## ACKNOWLEDGEMENTS

The authors wish to thank S. Herzberger for expert technical support and Jan Rojas for a critical review of the manuscript. Exploratory work leading to **5M** that was performed by Judith Hinck (and reproduced by the first author) is gratefully acknowledged. Financial support by DFG (grants RI 1063/1–2, RI 1063/4–1 and FOR 434) is also acknowledged.

## REFERENCES

1. Fodor,S.P.A., Read,JL., Pirrung,M.C., Stryer,L., Lu,.A.T. and Solas,D. (1991) Light-directed, spatially addressable parallel chemical synthesis. *Science*, **251**, 767–773.
2. Lockhardt,D.J. and Winzeler,E.A. (2000) Genomics, gene expression and DNA arrays. *Nature*, **405**, 827–836.
3. Pirrung,M.C. (2002) How to make a DNA chip. *Angew. Chem.*, **114**, 1327–1341; *Angew. Chem. Int. Ed. Engl.*, **41**, 1277–1289.

4. Lee,I., Dombkowski,A.A. and Athey,B.D. (2004) Guidelines for incorporating non-perfectly matched oligonucleotides into target-specific hybridization probes for a DNA microarray. *Nucleic Acids Res.*, **32**, 681–690.
5. Urakawa,H., El Fantroussi,S., Smidt,H., Smoot,J.C., Tribou,E.H., Kelly,J.J., Noble,P.A. and Stahl,D.A. (2003) Optimization of single-base-pair mismatch discrimination in oligonucleotide microarrays. *Appl. Environm. Microbiol.*, **69**, 2848–2856.
6. Halushka,M.K., Fan,J.B., Bentley,K., Hsie,L., Shen,N., Weder,A., Cooper,R., Lipshutz,R. and Chakravarti,A. (1999) Patterns of single-nucleotide polymorphisms in candidate genes for blood-pressure homeostasis. *Nat. Genet.*, **22**, 239–247.
7. Kirk,B.W., Feinsod,M., Favis,R., Kliman,R.M. and Barany,F. (2002) Single nucleotide polymorphism seeking long term association with complex disease. *Nucleic Acids Res.*, **30**, 3295–3311.
8. Bleczinski,C.F. and Richert,C. (1999) Steroid-DNA interactions increasing stability, sequence-selectivity, DNA/RNA discrimination and hypochromicity of oligonucleotide duplexes. *J. Am. Chem. Soc.*, **121**, 10889–10894.
9. Siegmund,K., Steiner,U.E. and Richert,C. (2003) CHIPCHECK—a program predicting total hybridization equilibria for DNA binding to small oligonucleotide microarrays. *J. Chem. Inf. Comput. Sci.*, **43**, 2153–2162.
10. Hall,T.S., Pancoska,P., Riccelli,P.V., Mandell,K. and Benight,A.S. (2001) Sequence context and thermodynamic stability of a single base pair mismatch in short deoxyoligonucleotide duplexes. *J. Am. Chem. Soc.*, **123**, 11811–11812.
11. Kutyavin,I.V., Afonina,I.A., Mills,A., Gorn,V.V., Lukhtanov,E.A., Belousov,E.S., Singer,M.J. Walburger,D.K., Lokhov,S.G., Gall,A.A. *et al*. (2000) 3′-Minor groove binder-DNA probes increase sequence specificity at PCR extension temperatures. *Nucleic Acids Res.*, **28**, 655–661.
12. Yoshitomi,K.J., Jinneman,K.C. and Weagant,S.D. (2003) Optimization of a 3′-minor groove binder-DNA probe targeting the uidA gene for rapid identification of *Escherichia coli* O157: H7 using real-time PCR. *Mol. Cell. Probes*, **17**, 275–280.
13. Bonnet,G., Tyagi,S., Libchaber,A. and Kramer,F.R. (1999) Thermodynamic basis of the enhanced specificity of structured DNA probes. *Proc. Natl Acad. Sci. USA*, **96**, 6171–6176.
14. Kushon,S.A., Jordan,J.P., Sefert,J.L., Nielsen,H., Nielsen,P.E. and Armitage,B.A. (2001) Effect of secondary structure on the thermodynamics and kinetics of PNA hybridization of DNA hairpins. *J. Am. Chem. Soc.*, **123**, 10805–10813.
15. Li,Q.Q., Luan,G.Y., Guo,Q.P. and Liang,J.X. (2002) A new class of homogeneous nucleic acid probes based on specific displacement hybridization. *Nucleic Acids Res.*, **30**, e5.
16. Mouritzen,P., Nielsen,A.T., Pfundheller,H.M., Choleva,Y., Kongsbak,L. and Moller,S. (2003) Single nucleotide polymorphism genotyping using locked nucleic acid (LNA). *Expert Rev. Mol. Diagnost.*, **3**, 27–38.
17. Nguyen,H.K., Fournier,O., Asseline,U., Dupret,D. and Thuong,N.T. (1999) Smoothing of the thermal stability of DNA duplexes by using modified nucleosides and chaotropic agents. *Nucleic Acids Res.*, **27**, 1492–1498.
18. He,J., Becher,G., Budow,S. and Seela,F. (2003) Pyrazolo[3,4-d]pyrimidine nucleic acids: adjustment of the dA-dT to the dG-dC base pair stability. *Nucleosides Nucleotides Nucleic Acids*, **22**, 573–576.
19. Seela,F. and He,Y. (2003) 6-Aza-2′-deoxyisocytidine: synthesis, properties of oligonucleotides and base-pair stability adjustment of DNA with parallel orientation. *J. Org. Chem.*, **68**, 367–377.
20. Mokhir,A.A., Tetzlaff,C.N., Herzberger,S., Mosbacher,A. and Richert,C. (2001) Monitored selection of DNA-hybrids forming duplexes with capped terminal C:G base pairs. *J. Comb. Chem.*, **3**, 374–386.
21. Tuma,J. and Richert,C. (2003) Solution structure of a steroid-DNA complex with cholic acid residues sealing the termini of a Watson–Crick duplex. *Biochemistry*, **42**, 8957–8965.
22. Altman,R.K., Schwope,I., Sarracino,D.A., Tetzlaff,C.N., Bleczinski,C.F. and Richert,C. (1999) Selection of modified oligonucleotides with increased target affinity via MALDI-monitored nuclease survival assays. *J. Comb. Chem.*, **1**, 493–508.
23. Bannwarth,W., Schmidt,D., Stallard,R.L., Hornung,C., Knorr,R. and Müller,F. (1988) Bathophenanthroline-ruthenium(II) complexes as non-radioactive labels for oligonucleotides which can be measured by time-resolved fluorescence techniques. *Helv. Chim. Acta*, **71**, 2085–2099.
24. Bannwarth,W. (1988) Solid phase synthesis of oligodeoxynucleotides containing phosphoramidate internucleotide linkages and their specific chemical cleavage. *Helv. Chim. Acta.*, **71**, 1517–1527.
25. Tetzlaff,C.N., Schwope,I., Bleczinski,C.F., Steinberg,J.A. and Richert,C. (1998) A convenient synthesis of 5′-amino-5′-deoxythymidine and preparation of peptide-DNA hybrids. *Tetrahedron Lett.*, **39**, 4215–4218.
26. Mag,M. and Engels,J.W. (1989) Synthesis and selective cleavage of oligodeoxynucleotides containing non-chiral internucleotide phosphoramidate linkages. *Nucleic Acids Res.*, **17**, 5973–5988.
27. Berlin,K., Jain,R.K., Tetzlaff,C., Steinbeck,C. and Richert,C. (1997) Spectrometrically monitored selection experiments: quantitative laser desorption mass spectrometry of small chemical libraries. *Chem. Biol.*, **4**, 63–77.
28. Connors,W.H., Narayanan,S., Kryatova,O.P. and Richert,C. (2003) Synthesis of oligonucleotides with a 2′-cap at the 3′-terminus via reversed phosphoramidites. *Org. Lett.*, **5**, 247–250.
29. Tuma,J. Connors,W.H., Stitelman,D.H. and Richert,C. (2002) On the effect of covalently appended quinolones on termini of DNA-duplexes. *J. Am. Chem. Soc.*, **124**, 4236–4246.
30. Kool,E.T, Morales,J.C. and Guckian,K.M. (2000) Mimicking the structure and function of DNA: insights into DNA stability and replication. *Angew. Chem. Int. Ed. Engl.*, **39**, 990–1009.
31. Smirnov,S., Matray,T.J., Kool,E.T. and de los Santos,C. (2002) Integrity of duplex structures without hydrogen bonding: DNA with pyrene paired at abasic sites. *Nucleic Acids Res.*, **30**, 5561–5569.
32. Guckian,K.M., Schweitzer,B.A., Ren,R.X.F., Sheils,C.J., Paris,P.L., Tahmassebi,D.C. and Kool,E.T. (1996) Experimental measurement of aromatic stacking affinities in the context of duplex DNA. *J. Am. Chem. Soc.*, **118**, 8182–8183.
33. Rosemeyer,H. and Seela,F. (2002) Modified purine nucleosides as dangling ends of DNA duplexes: the effect of the nucleobase polarizability on stacking interactions. *J. Chem. Soc., Perkin Trans.*, **2**, 746–750.
34. Freier,S.M., Burger,B.J., Alkema,D., Neilson,T. and Turner,D.H. (1983) Effects of 3′ dangling end stacking on the stability of GGCC and CCGG double helices. *Biochemistry*, **22**, 6198–6206.
35. Ren,R.X.F., Chaudhuri,N.C., Paris,P.L., Rumney,S. and Kool,E.T. (1996) Naphthalene, phenanthrene and pyrene as DNA base analogues: synthesis, structure and fluorescence in DNA. *J. Am. Chem. Soc.*, **118**, 7671–7678.
36. Beuck,C., Singh,I., Bhattacharya,A., Hecker,W., Parmar,V.S., Seitz,O. and Weinhold,E. (2003) Polycyclic aromatic DNA-base surrogates: high-affinity binding to an adenine-specific base-flipping DNA methyltransferase. *Angew. Chem. Int. Ed.*, **42**, 3958–3960.
37. Bommarito,S., Peyret,N. and SantaLucia,J. (2000) Thermodynamic parameters for DNA sequences with dangling ends. *Nucleic Acids Res.*, **28**, 1929–1934.
38. Dogan,Z., Paulini,R., Rojas Stütz,J.A., Narayanan,S. and Richert,C. (2004) 5′-Tethered stilbene derivatives as fidelity- and affinity-enhancing modulators of DNA duplex stability. *J. Am. Chem. Soc.*, **126**, 4762–4763.
39. Guo,Z., Liu,Q. and Smith,L.M. (1997) Enhanced discrimination of single nucleotide polymorphisms by artificial mismatch hybridization. *Nat. Biotechnol.*, **15**, 331–335.